A high-magnetic-field-induced density-wave state in graphite

2009 J. Phys.: Condens. Matter 21 344207

(http://iopscience.iop.org/0953-8984/21/34/344207)

J. Phys.: Condens. Matter **21** (2009) 344207 (7pp) doi:10.1088/0953-8984/21/34/344207

A high-magnetic-field-induced density-wave state in graphite

Hiroshi Yaguchi[1] **and John Singleton**[2]

[1] Department of Physics, Faculty of Science and Technology, Tokyo University of Science, Noda 278-8510, Japan
[2] National High Magnetic Field Laboratory, LANL, MS-E536, Los Alamos, NM 87545, USA

Received 22 May 2009, in final form 1 July 2009
Published 27 July 2009
Online at stacks.iop.org/JPhysCM/21/344207

Abstract
Whilst the realization of graphene, probably one of the best two-dimensional carrier systems to study, has attracted much research interest recently, graphite, which may be regarded as multi-layered graphene, has also been known to exhibit very interesting phenomena at high magnetic fields and low temperatures. The electron–hole system in the compensated semimetal graphite undergoes a magnetic-field-induced electronic phase transition and successive transitions, including a reentrant transition back to the normal phase, at higher magnetic fields. In this article, we review the physics of the high-magnetic-field phase of graphite and elaborate on our studies on this subject using pulsed high magnetic fields.

1. Introduction

Graphite is a semimetal with a layered structure. Each single layer, well known as graphene, comprises of a planar hexagonal network of carbon atoms bonded by three of the four valence electrons in sp^2 hybrid orbitals, with the remaining electron in the p_z orbital forming a π-type molecular orbital. Graphene is intrinsically a zero-gap semiconductor since the Fermi level crosses at the K (K′) point (or the Dirac point), where the conduction band (anti-bonding π band) and the valence band (bonding π band) are tangent. By contrast, graphite is a semimetal due to the bonding and anti-bonding π bands overlapping, giving rise to electrons near the K (K′) point and holes near the H (H′) point; the electron and hole carrier densities being very small ($n = p \approx 3 \times 10^{18}$ cm^{-3}) compared to those of typical metals [1].

The electron- and hole-Fermi surfaces are located along the vertical H–K–H (H′–K′–H′) edge in the hexagonal Brillouin zone. Since the two Brillouin zone edges, labelled H–K–H and H′–K′–H′, are non-equivalent, these π bands are degenerate in energy. The Fermi surfaces are much elongated, which makes the in-plane effective masses very light ($\sim$0.05 m_e) and, in contrast, the inter-plane masses rather large ($\sim$10 m_e). The small in-plane masses and low carrier density conspire to allow the carrier system to be in its quantum limit at moderate magnetic fields parallel to the c-axis or normal to the basal plane. The large inter-plane masses lead to an enhancement of the density of states at the Fermi level. These circumstances contrive to ensure that the carrier system may be greatly affected by the application of even moderate magnetic field.

The first experimental indication of such a phenomenon was obtained as the observation of an abrupt increase in the low-temperature magnetoresistance caused by the application of a magnetic field parallel to the c-axis [2]. Since then, a number of experimental studies using either steady or pulsed magnetic fields have been made to elucidate the nature of the magnetic-field-induced phase with the resistance anomaly as its onset. The sharpness of the resistance increase and the strong dependence of its onset field on temperature strongly suggest that it be interpreted as an electronic phase transition involving many-body effects [3]. Whereas the real nature of this phenomenon still remains unknown, the magnetic-field-induced phase has been theoretically discussed in terms of the formation of a density wave caused by $2k_F$-type nesting [4]. Such a theoretical study naturally led to the idea that there will be successive transitions of a similar nature and/or a reentrant transition back to the normal state at higher fields. In fact, our pulsed-magnetic-field study conducted later obtained definitive evidence of a reentrant transition [5]. We shall refer to the magnetic-field-induced phase as the (field-induced) density-wave state for convenience.

2. High-magnetic-field phase of graphite

2.1. Field-induced electronic phase transition and reentrant transition

As briefly described above, the electron–hole system in graphite undergoes a magnetic-field-induced electronic phase

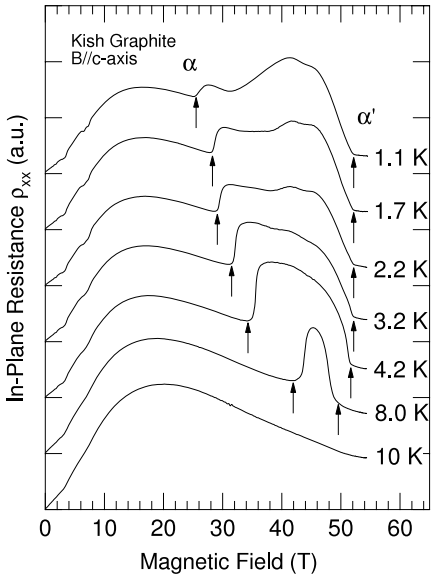

Figure 1. Transverse magnetoresistance ρ_{xx} at different temperatures between 1.1 and 10 K. The onset transition (α) and the reentrant transition (α') are indicated with arrows. Shubnikov–de Haas oscillations are seen around 3 and 7 T at low temperatures.

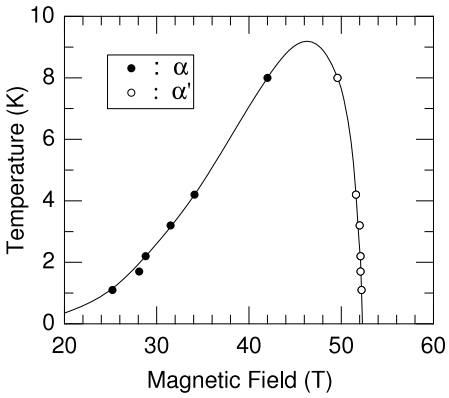

Figure 2. Phase diagram of graphite in the H–T plane. The solid circles represent data points of the onset (α) field, and the open circles represent the reentrant (α') transition. The solid curve through the data points is a guide to the eye and provides an approximation to the phase boundary.

transition accompanied by a resistance increase as the onset [3]. In most experimental studies on this subject done thus far, Kish graphite [6, 7] has been chosen. Indeed, all of the graphite samples used in the studies described in this article were flakes of Kish graphite. Kish graphite, which is artificially grown by precipitation from carbon-saturated molten iron or nickel [6, 7], has been found to exhibit the onset of the field-induced density-wave state in a consistent manner. In contrast, samples such as highly orientated pyrolytic graphite (HOPG), which is polycrystalline graphite with ordered c-axis orientation, are seen to exhibit somewhat poor features associated with the field-induced phase transition, and do not appear to behave very reproducibly from sample to sample [3]. Such a difference between Kish graphite and HOPG is perhaps due to the dimensionality. In fact, this idea is supported by recent magnetoresistance measurements [8] and scanning tunnelling spectroscopy (STS) experiments in magnetic fields [9]. The magnetoresistance experiments signal the occurrence of the (integer) quantum Hall effect, which is inherent in the two-dimensional system, in HOPG samples (but not in Kish graphite samples) [8]. The STS measurements in magnetic fields parallel to the c-axis [9] indicated that Kish graphite is identified as bulk graphite whilst HOPG may be regarded as graphite with a finite thickness of about 40 layers. Both of these studies strongly suggest that HOPG is considerably more two-dimensional than Kish graphite.

Our pulsed-magnetic-field study revealed that the onset transition to the field-induced density-wave state is, at a higher field, followed by a reentrant transition back to the normal state [5]. Figure 1 shows the transverse magnetoresistance ρ_{xx} in pulsed magnetic fields of ∼55 T at various temperatures. For all the temperatures except 10 K, a sharp resistance increase is clearly seen (labelled α, after [10]), which is the feature attributed to the electronic phase transition to the field-induced density-wave state mentioned above [2, 3]. The resistance then exhibits complicated behaviour, particularly at low temperatures and drops dramatically at fields higher than ∼45 T. Eventually, the resistance shows a sharp bend around 50 T (labelled α' in figure 1) and approaches an extrapolation of the resistance from below the onset field. This is a very strong indication of a reentrant transition to the normal phase. The width between the α and α' fields becomes narrower with increasing temperature and no discernible structures attributable to the transitions can be seen at or above 10 K. The attribution of α' to a reentrant transition leads to the proposed phase diagram for graphite shown in figure 2. A smooth solid curve is employed through the data points as a guide to the eye and represents an approximation of the phase boundary between the ordered state and the normal state.

In order to understand the phase diagram in the H–T plane (magnetic-field–temperature plane), let us first focus on the temperature dependence of the onset field. The onset field at liquid helium temperatures is typically 20–30 T; this field range was intensively investigated using steady magnetic field to determine accurately the phase boundary in the H–T plane [3, 11] in the early stage of the research. At least in this field range, the relationship between the critical temperature and the applied field was found to be empirically expressed by the formula

$$T_c(B) = T^* \exp\left(-\frac{B^*}{B}\right), \tag{1}$$

where T^* and B^* are adjustable parameters. This empirical formula was inspired by the Bardeen–Cooper–Schrieffer (BCS)-type formula for a mean-field-type pairing transition

$$k_B T_c(B) = 1.14 E_F \exp\left(-\frac{1}{N(E_F)V}\right), \tag{2}$$

where $N(E_F)$ is the density of states at the Fermi level and V is the relevant pairing interaction. The values of T^* obtained in existing experimental studies are of the order of the Fermi energy of graphite (∼20 meV) in accordance

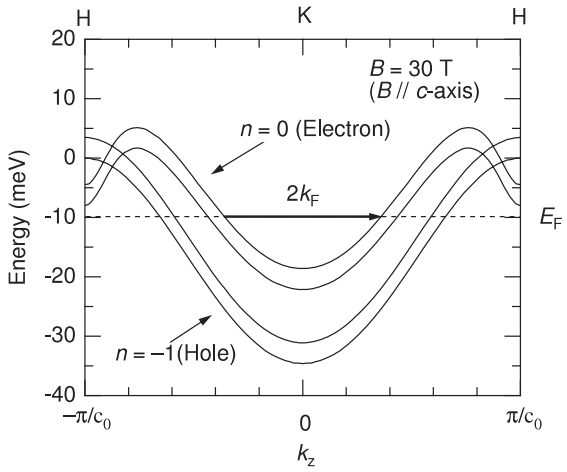

Figure 3. Landau levels of graphite in a magnetic field of 30 T parallel to the c-axis. The nesting vector for the charge density wave in the $n = 0$, spin-up subband is shown as an example.

with equation (2) [3, 10–12]. (In reality, the Fermi energy depends on magnetic field. Its field dependence does play a very important role in the occurrence of the reentrant transition at higher fields. For this field range, nevertheless, the magnetic field dependence of the Fermi energy is modest, and consequently T^* in equation (1) may be approximated to be constant.) The applied field B in the exponent in equation (1) reflects that the density of states at the Fermi level is proportional to the field B owing to the Landau degeneracy factor. In support of the validity of the empirical formula, the pressure effect on the transition temperature was found to be explained by equation (1) taking into account the changes in the density of states and the bandwidth (Fermi energy) by the application of pressure [13].

Meanwhile, Yoshioka and Fukuyama (YF) [4] proposed a model (see also [11]) which ascribes the resistance increase to a charge-density-wave (CDW) instability due to the quasi-one-dimensionality of the energy spectrum caused by Landau quantization. In high magnetic fields in excess of 7.4 T, the carrier system in graphite is in its quasi-quantum limit, where only the lowest electron ($n = 0$) and hole ($n = -1$) Landau subbands (each of them spin-split) are populated. In the field range of interest (magnetic field $B > 20$ T), all the other subbands of higher index are far away from the Fermi level; under such conditions, several nestings across two Fermi points are possible at low enough temperatures [4, 11]. (Figure 3 illustrates the Landau subband dispersion at $B = 30$ T, which is a typical magnetic field strength for the phenomenon to be discussed [3].)

YF calculated the transition temperatures of possible $2k_F$-type instabilities (e.g. charge- or spin-density-wave instabilities) and concluded that of the CDW associated with the $n = 0$ spin-up subband is the highest [4], giving the transition temperature as

$$k_B T_c(B) = 4.53 E_F \frac{\cos^2(\frac{1}{2}c_0 k_{F0\uparrow})}{\cos(c_0 k_{F0\uparrow})} \exp\left(-\frac{2}{N_{0\uparrow}(E_F)u(\epsilon)}\right), \quad (3)$$

where E_F is the Fermi energy (i.e. the occupied energy width of the relevant Landau subband), $k_{F0\uparrow}$ is the Fermi wavevector of the $n = 0$ spin-up subband, c_0 is the lattice constant along the c-axis, $N_{0\uparrow}(E_F)$ is the density of states of the $n = 0$ spin-up subband at the Fermi level (chemical potential). u is the relevant pairing interaction as a function of the dielectric constant ϵ. E_F, $k_{F0\uparrow}$, $N_{0\uparrow}(E_F)$ and u all depend on magnetic field B. The dielectric constant ϵ is treated as the only adjustable parameter in equation (3) [11].

In this scenario, YF suggest that two sets of CDWs that are out of phase with each other can be stabilized without the Hartree energy loss (the direct Coulomb interaction) [4] owing to the existence of the doubly degenerate subbands located along the H–K–H and H′–K′–H′ edges[3]. In view of this, therefore, such a density wave perhaps should be called a *valley* density wave (VDW) rather than simply a CDW. YF also point out that the electron–phonon interaction is several orders of magnitude smaller than the relevant interaction [4]; the CDW is driven by the (exchange) Coulomb interaction. In addition, this type of CDW is spin-polarized, so that increasing the applied field is not liable to suppress the nesting via the Zeeman (Pauli) effect, unlike a CDW pre-existing in zero magnetic field, which occurs in both spin-up and spin-down subbands simultaneously [14].

Although equation (3) is derived for a particular $2k_F$-type instability, its functional form is, as discussed in [11], identical to those for the other possible $2k_F$-type instabilities and is very similar to that of the general BCS-type formula equation (2). In order for the higher-field region to be understood, the field dependence of the Fermi energy is indeed important. Whereas the exponent in equation (3) (or equation (2)) increases with increasing magnetic field, the pre-exponential decreases owing to the field dependence of the Fermi energy. The Fermi energy associated with the $n = 0$ spin-up Landau subband decreases with magnetic field, and is expected to reach zero at a field higher than 60 T according to band calculations based on the Slonczewski–Weiss–McClure (SWM) model [15, 16]. This corresponds to the $n = 0$ spin-up Landau subband crossing the Fermi level, so that no carriers remain in the subband above the crossing field B_{cross}. The transition temperature $T_c(B)$ therefore tends to zero as the Fermi energy approaches zero because T_c is proportional to the Fermi energy in equation (3) (or equation (2)). In other words, the reentrant transition field should extrapolate to B_{cross} at zero temperature. Therefore, at least in a qualitative fashion, the mechanism for the reentrant transition may be understood along this line of discussion.

Since band calculations based on the SWM model indicate that the $n = 0$ spin-up Landau subband crosses the Fermi level at a field higher than 60 T, the combination of the YF theory (or equation (3)) and the SWM model leads to the idea that the reentrant transition will occur above 60 T at zero temperature, showing a discrepancy between theory and experiment [5]. Takada and Goto [17] calculated the renormalized band structure on the basis of the SWM model by taking into account

[3] Takahashi and Takada's study on the single-electron wavefunctions revealed that electrons in the H–K–H edge and those in the H′–K′–H′ edge reside mostly in adjacent layers in real space, so that the Hartree term is not completely cancelled [19].

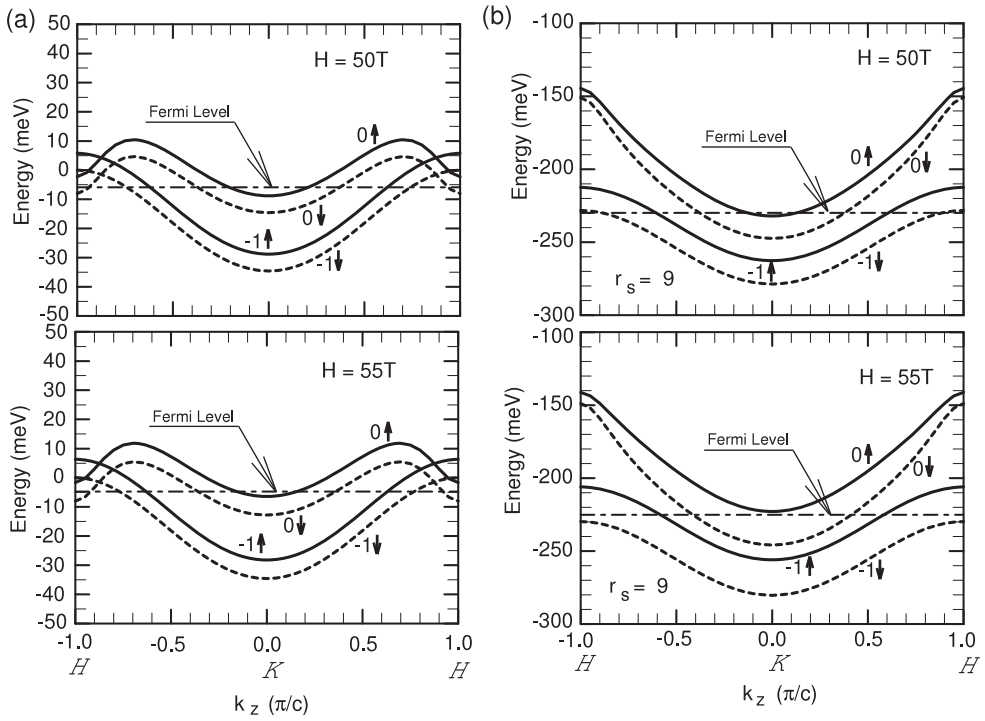

Figure 4. Electronic structure of graphite at fields of 50 and 55 T. In (a), no many-body effect is considered, whilst in (b), the self-energy correction is included self-consistently (reprinted from [17] by Takada and Goto with permission). (a) SW energy dispersion. (b) With self-energy correction.

self-energy corrections, and revealed the importance of such corrections in the vicinity of the crossing field. They found that the $n = 0$ spin-up and $n = -1$ spin-down Landau subbands cross the Fermi level, upwards and downwards respectively, almost simultaneously at ∼53 T. By contrast, those Landau subbands are occupied at the same field in the conventional band calculations based on the SWM model (figure 4). This implies that T_c should go to zero at the same field, in excellent agreement with the experimental observations [5] (see figure 2; the reentrant transition extrapolates to $B \approx 52.3$ T at zero temperature). Takada and Goto's calculations [17] also suggest that the bandwidth collapses rapidly to zero as the crossing field is approached. Since the transition temperature given by equation (3) is proportional to the Fermi energy, this explains the very steeply falling high-field side of the phase boundary in figure 2.

The agreement between the predictions of Takada and Goto [17] and the experiment [5] provides strong support for the reentrant transition being a consequence of a Landau subband crossing the Fermi level. The transition may be associated with the $n = 0$ spin-up and/or $n = -1$ spin-down subband, as both cross the Fermi level almost simultaneously at about 53 T in Takada and Goto's calculations [17]; therefore, the exact nature of the electronic state between the α and α' boundaries remains somewhat uncertain. In this context, it should be noted that other theoretical work made subsequent to the YF theory reached different conclusions as to which of the possible nesting instabilities has the highest critical temperature (e.g. a CDW in the $n = -1$ subband [18]; a spin density wave (SDW) in the $n = 0$ subband [19]).

2.2. Properties of the field-induced density-wave phase

2.2.1. Possible successive phase transition. As can be seen in figure 1, the in-plane (transverse) magnetoresistance ρ_{xx} shows rather complicated behaviour above the α transition at low temperatures (below ∼3 K). This is particularly evident in the 1.1 K trace in figure 1; the resistance increases twice between the α and α' transitions (see inset to figure 5). Figure 5 demonstrates that this behaviour becomes much more evident in the out-of-plane (longitudinal) magnetoresistance ρ_{zz} in a close temperature range (below ∼3 K). These features in ρ_{xx} and ρ_{zz} probably correspond to each other, which is labelled β after [10]. (The 1.1 K trace in the inset to figure 5 is taken from figure 1.) This resistance increase labelled β also might signal another $2k_F$-type transition. It is noteworthy that with decreasing temperature the feature associated with β becomes more pronounced and the feature associated with α becomes attenuated. This might be a consequence of the two phases preceded by α and by β competing with each other.

In [20], the out-of-plane (longitudinal) magnetoresistance ρ_{zz} was investigated in magnetic fields of up to ∼37 T and a steep resistance increase in ρ_{zz} was found at low temperatures. Besides this, it was found that the steep resistance increase is accompanied by non-ohmic transport, which may be interpreted as the sliding of a depinned density wave along the c-axis. In contrast, Iye and Dresselhaus [21] found non-ohmic transport in the in-plane (transverse) magnetoresistance ρ_{xx} in the phase immediately after the α transition, which leads to the α transition being interpreted as a density-wave transition *perpendicular* to the c-axis rather than *parallel* to

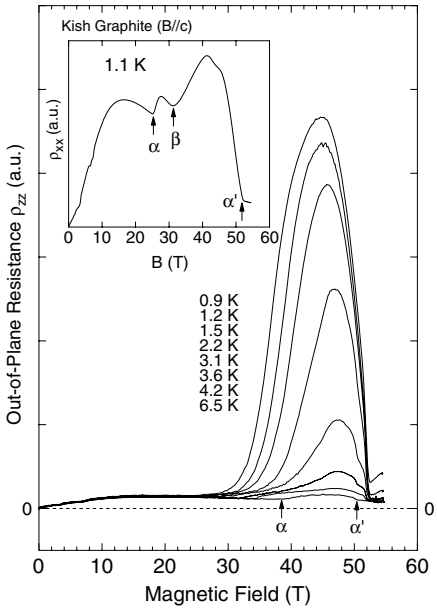

Figure 5. Longitudinal magnetoresistance ρ_{zz} at various temperatures. The onset transition (α) and the reentrant transition (α') at 6.5 K are indicated with arrows. The inset shows the transverse magnetoresistance ρ_{xx} at 1.1 K for comparison; the α, β and α' transitions are indicated with arrows.

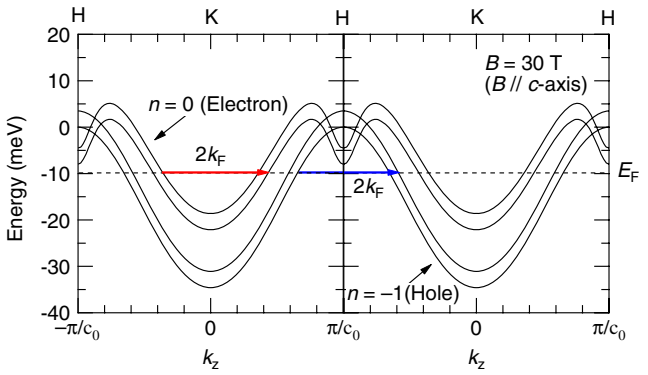

Figure 6. Landau levels of graphite in a magnetic field of 30 T parallel to the c-axis in the extended zone representation. The nesting vector for the SDW common to the $n = 0$ (red) and $n = -1$ (blue) subbands is shown.

(This figure is in colour only in the electronic version)

the c-axis. As the directions in which the two kinds of non-ohmic transport [20, 21] are very different, these observations also suggest the occurrence of two distinct phases. In view of the directions of the density waves, the β transition fits YF's theoretical model of a $2k_F$-type instability along the c-axis better than the α transition does.

Also, if any of the Landau subbands remain unnested in the phase whose onset is the β transition, the steep increase in the out-of-plane magnetoresistance ρ_{zz} associated with the β transition would be significantly reduced. In order for all the Landau subbands to be nested simultaneously, the only possible nesting vector common to all the occupied Landau subbands is that for the SDW, i.e. connecting two Fermi points via $k_z = 0$ for the electron subband and via $k_z = \pi/c_0$ in the extended zone representation for the hole subbands (figure 6), or vice versa. The charge neutrality in a compensated semimetal ensures that the nesting vectors for the electron and hole bands are translationally equivalent in the extended zone representation. (A slightly more detailed explanation about the translational equivalence of the two subbands will be given in section 2.2.2.)

2.2.2. Hole doping by neutron irradiation. As graphite is a compensated semimetal, the concentrations of electrons and of holes are ideally the same. In other words, the charge neutrality condition determines the Fermi level and the Fermi wavevectors k_F in the occupied Landau subbands. Therefore, carrier doping will certainly affect the density-wave state. Fast-neutron irradiation creates lattice defects, some of which act as acceptors [22]. In order to gain insight into which Landau subband and which instability are relevant for the magnetic-field-induced density-wave state, we have used samples that were irradiated with fast neutrons of a flux ($E > 1$ MeV) of 5.5×10^{12} cm^{-2} s^{-1} at 50 °C for 1, 2 and 4 h in JAERI JRR-4. (The imbalances of the electron and hole densities $p - n$ are estimated to be 0.7, 1, 2×10^{18} cm^{-3} from Hall measurements, respectively.)

Figure 7 shows the transverse magnetoresistance ρ_{xx} of neutron-irradiated graphite in pulsed magnetic fields of ~53 T at different temperatures; at all the temperatures, both the onset transition α and the reentrant transition α' are observed. Figure 8 displays the phase diagram of neutron-irradiated graphite in the H–T plane. With increasing neutron dosage, the onset transition α shifts towards higher fields whilst the reentrant transition α' shifts towards lower fields. The increase of the onset field (α) with dosage (or hole doping) has been explained as a manifestation of the pair-breaking effect on a pairing transition such as a density-wave transition due to the increased scattering [22]. (The increased scattering causing the pair-breaking effect was not intentional, but was a sort of side effect of hole doping by neutron irradiation.)

As described previously in section 2.1, the reentrant transition may be understood as a consequence of Fermi level crossing (or depopulation) of the Landau subband(s) responsible for the field-induced density-wave state [5]. For neutron-irradiated specimens as well as the pristine one, the extrapolation of the reentrant field to zero temperature probably gives a good approximation to the field at which the relevant Landau subband crosses the Fermi level. Such an extrapolated field shifts towards lower fields with neutron irradiation dosage (or hole doping). This provides strong evidence for the involvement of the electron ($n = 0$) subband with the field-induced density-wave state, because each electron (hole) Landau subband's crossing field should move to a lower (higher) field with hole doping. However, it should be noted that the possibility of the participation of the hole ($n = -1$) subband in the field-induced state is not necessarily excluded.

The other thing to mention in terms of the results in figure 7 will be the disappearance (or strong suppression) of the β transition. Whilst the α transition appears even in the sample

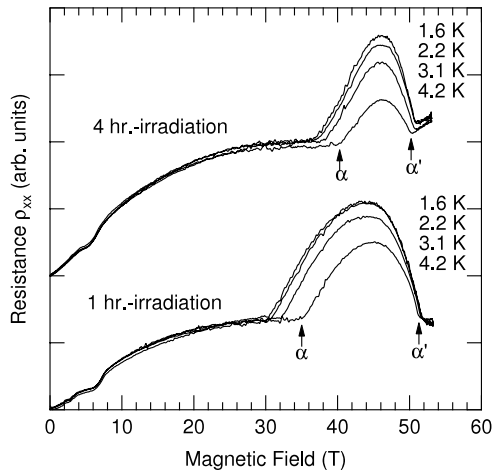

Figure 7. Magnetoresistance traces of neutron-irradiated specimens. The onset transition (α) and the reentrant (α') transition at 4.2 K are indicated with arrows. Whilst the α and the α' transitions are rather robust against irradiation, the β transition disappears.

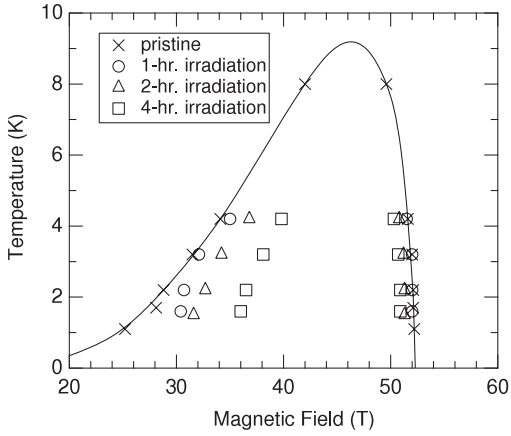

Figure 8. Phase diagram of pristine and neutron-irradiated graphite in the H–T plane. The open symbols denote the onset (α) and reentrant (α') fields of neutron-irradiated graphite. The crosses represent those for pristine graphite. The solid curve through the crosses is a guide to the eye and provides an approximate phase boundary for pristine graphite.

with the highest dose, the β transition does not appear in any of the three neutron-irradiated samples. We have confirmed that the β transition does not occur even in fields of up to ~53 T. We suggest that this might provide evidence for the β transition corresponding to the SDW transition. Since the energy spectrum in magnetic field is one-dimensional owing to Landau quantization, this charge neutrality condition may be expressed as

$$k_{\mathrm{F}(n=0,\uparrow)} + k_{\mathrm{F}(n=0,\downarrow)} + k_{\mathrm{F}(n=-1,\uparrow)} + k_{\mathrm{F}(n=-1,\downarrow)} = \frac{2\pi}{c_0}, \quad (4)$$

where k_{F} is the Fermi wavevector of each Landau subband and c_0 is the lattice constant along the c-axis. Therefore, as illustrated in figure 6, the nesting vectors associated with the SDW may be taken to be $k_{\mathrm{F}(n=0,\uparrow)} + k_{\mathrm{F}(n=0,\downarrow)} = (\frac{\pi}{c_0} - k_{\mathrm{F}(n=-1,\uparrow)}) + (\frac{\pi}{c_0} - k_{\mathrm{F}(n=-1,\downarrow)})$ for both the electron subbands and the hole subbands. In other words, the formation of the SDW relies on the charge neutrality condition (equation (4)). Therefore the suppression of the β transition could be due to the violation of the charge neutrality condition, equation (4), in the neutron-irradiated samples.

2.3. *Other features of the field-induced density-wave phase*

As partially mentioned above, there is other evidence for the field-induced state being a density-wave state.

2.3.1. Field- and frequency-dependent transport. Both in a CDW state and in an SDW state, field- and frequency-dependent transport due to sliding motion of the depinned density wave can be observed [23, 24].

Iye and Dresselhaus reported non-ohmicity in the conduction parallel to the ab-plane, reminiscent of depinning of a density wave, at magnetic fields between the α and the β transitions; a typical threshold electric field was ~100 mV cm^{-1} [21]. Later, Yaguchi *et al* observed non-ohmicity in the conduction parallel to the c-axis, attributable to depinning of a density wave, at magnetic fields above the β transitions; a typical threshold electric field being ~1 V cm^{-1} [20]. The discrepancy between these two studies probably comes from the phases where non-ohmic conduction was observed as being different.

Nakamura and co-workers investigated the resistance anomaly associated with the onset transition by DC and AC measurements and found that the resistance around the transition is frequency dependent [25]. However, the onset magnetic field of the density-wave state hardly depends on measurement frequency. Subsequently, Takamasu and co-workers made a more systematic study at frequencies of up to 10 MHz, and found that the frequency dependence of the real and imaginary parts of the conductivity are explained in terms of a phenomenological model for a conventional one-dimensional conductor [26].

2.3.2. Pair-breaking effect on the formation of a density wave. As superconductivity is caused by electron–electron pairing, both a CDW and an SDW are caused by electron–hole pairing. Similar to magnetic impurities in an s-wave superconductor in the Abrikosov–Gor'kov theory [27], charged (ionized) impurities in a density-wave system act as pair-breakers [28, 29]. The pair-breaking effect due to the relevant impurity scattering reduces the critical temperature (or increases the transition field for the present case in graphite) and may be expressed by the equation

$$\ln\left(\frac{T_{\mathrm{c}}}{T_{\mathrm{c0}}}\right) = \Psi\left(\frac{1}{2}\right) - \Psi\left(\frac{1}{2} + \frac{\hbar}{2\pi\tau k_{\mathrm{B}} T_{\mathrm{c}}}\right), \quad (5)$$

where T_{c0} is the critical temperature in the absence of the pair-breaking effect and Ψ is the digamma function. τ is the scattering time associated with the pair-breaking process, which may be treated as an adjustable parameter.

For the field-induced density-wave transition in graphite, the suppression of the critical temperature due to an increase

of scattering was reported in samples containing ionized impurities acting as donors (typically $n - p \approx 1 \times 10^{16}$ cm^{-3}) [30], and in neutron-irradiated samples (typically $p - n \approx 1 \times 10^{18}$ cm^{-3}) [22] where lattice defects created by the neutron irradiation act as acceptors. In either case, the reduction of the critical temperature was explained in terms of the pair-breaking effect using equation (5) with a reasonable choice of a value for the adjustable parameter τ.

3. Summary

The carrier system in graphite undergoes magnetic-field-induced electronic phase transitions. This phenomenon is often discussed in terms of the formation of a $2k_F$-type density wave along the c-axis, and is explained rather successfully, whereas the real nature of the density-wave state still remains somewhat unclear. We have mainly described our studies on this subject using pulsed magnetic fields of over 50 T. We obtained a definitive indication of a reentrant transition back to the normal state owing to the Landau subbands crossing the Fermi level (depopulation of the subband), and demonstrated the importance of the self-energy effect in the vicinity of the crossing field. We have also discussed a successive transition in terms of the possible formation of a SDW.

Finally, we suggest that the occurrence of the field-induced density-wave state relies on the following fortuitous circumstances characteristic of graphite.

- Low carrier densities and small in-plane masses, which lead to the electronic system being in its (quasi-) quantum limit at moderate magnetic fields.
- Large effective masses along the c-axis, which lead to a large enhancement of the density of states at the Fermi level.
- Charge neutrality condition in a compensated semimetal, which makes the electron-and hole-Landau subbands translationally equivalent.
- Valley degeneracy (H–K–H and H′–K′–H′), which might play an important role in the formation of a CDW (or VDW) with the reduction of the Hartree energy loss.

These conditions make the carrier system in graphite somewhat special and very intriguing in high magnetic fields.

Acknowledgments

We thank Y Iye, T Takamasu, N Miura, T Iwata, H Jones, T Hickman and Y Takada for their invaluable support and discussions. Part of this work was supported by EPSRC (UK) and the Japan Society for the Promotion of Science (JSPS).

References

[1] Brandt N B, Chudinov S M and Ponomaev Ya G (ed) 1988 *Semimetals* vol 1 *Graphite and its Compounds* (Amsterdam: North-Holland)
[2] Tanuma S, Inada R, Furukawa A, Takahashi O and Iye Y 1981 *Physics in High Magnetic Fields* ed S Chikazumi and N Miura (New York: Springer) p 316
[3] Iye Y, Tedrow P M, Timp G, Shayegan M, Dresselhaus M S, Dresselhaus G, Furukawa A and Tanuma S 1982 *Phys. Rev.* B **25** 5478
[4] Yoshioka D and Fukuyama H 1981 *J. Phys. Soc. Japan* **50** 725
[5] Yaguchi H and Singleton J 1998 *Phys. Rev. Lett.* **81** 5193
[6] Austerman S B 1968 *Chemistry and Physics of Carbon* vol 4 ed P L Walker and P A Thrower (New York: Dekker) p 137
[7] Takezawa T, Tsuzuku T, Ono A and Hishiyama Y 1969 *Phil. Mag.* **19** 623
[8] Kopelevich Y, Torres J H S, da Silva R R, Mrowka F, Kempa H and Esquinazi P 2003 *Phys. Rev. Lett.* **90** 156402
[9] Matsui T, Kambara H, Niimi Y, Tagami K, Tsukada M and Fukuyama H 2005 *Phys. Rev. Lett.* **94** 226403
[10] Yaguchi H, Iye Y, Takamasu T and Miura N 1993 *Physica* B **184** 332
[11] Iye Y, Berglund M and McNeil L E 1984 *Solid State Commun.* **52** 975
[12] Ochimizu H, Takamasu T, Takeyama S, Sasaki S and Miura N 1992 *Phys. Rev.* B **46** 1986
[13] Iye Y, Murayama C, Môri N, Yomo S, Nicholls J T and Dresselhaus G 1990 *Phys. Rev.* B **41** 3249
[14] Brooks J S 2008 *Rep. Prog. Phys.* **71** 126501
[15] Slonczewski J C and Weiss P R 1958 *Phys. Rev.* **109** 272
[16] McClure J W 1960 *Phys. Rev.* **119** 606
[17] Takada Y and Goto H 1998 *J. Phys.: Condens. Matter* **10** 11315
[18] Sugihara K 1984 *Phys. Rev.* B **29** 6722
[19] Takahashi K and Takada Y 1994 *Physica* B **201** 384
[20] Yaguchi H, Takamasu T, Iye Y and Miura N 1999 *J. Phys. Soc. Japan* **68** 181
[21] Iye Y and Dresselhaus G 1985 *Phys. Rev. Lett.* **54** 1182
[22] Yaguchi H, Iye Y, Takamasu T and Miura N 1999 *J. Phys. Soc. Japan* **68** 1300
[23] Grüner G 1988 *Rev. Mod. Phys.* **60** 1129
[24] Grüner G 1994 *Rev. Mod. Phys.* **66** 1
[25] Nakamurai K, Osada T, Kido G, Miura N and Tanuma S 1983 *J. Phys. Soc. Japan* **52** 2875
[26] Takamasu T, Ochimizu H and Miura N 1993 *Physica* B **184** 327
[27] Abrikosov A A and Gor'kov L P 1960 *Zh. Eksp. Teor. Fiz.* **39** 1781
Abrikosov A A and Gor'kov L P 1961 *Sov. Phys.—JETP* **12** 1243 (Engl. Transl.)
[28] Zittartz J 1967 *Phys. Rev.* **164** 575
[29] Gómez-Santos G and Ynduráin F 1984 *Phys. Rev.* B **29** 4459
[30] Iye Y, McNeil L E and Dresselhaus G 1984 *Phys. Rev.* B **30** 7009